

# DATA FUSION OF MULTI-SOURCE REMOTE SENSING BASED ON LEVEL SET METHOD AND APPLICATION TO URBAN ROAD EXTRACTION

Cao Guangzhen<sup>a, \*</sup>, Hou Peng<sup>b</sup>, Jin Ya-Qiu<sup>c</sup>

<sup>a</sup> Key Laboratory of Radiometric Calibration and Validation for Environmental Satellites, China Meteorological Administration (LRCVES/CMA), Beijing 100081, China – gzhencao@hotmail.com;

<sup>b</sup> Resources school, Beijing Normal University, Beijing 100875, China – houpcy@163.com;

<sup>c</sup> The Key Laboratory for Wave Scattering and Remote Sensing Information (Ministry of Education) Fudan University, Shanghai 200433, China – yqjin@fudan.ac.cn

**KEY WORDS:** Urban; Multisensor; Fusion; Algorithms; Semi-automation; Extraction

## ABSTRACT:

Using data fusion of multi-spectral and microwave radar images, a semiautomatic method is developed based on the level set method for application to urban road extraction. The fast marching method of level set makes data fusion. Radar remote sensing image can make up road breaks due to shadowing of high building or tree canopy in multi-spectral image, while multi-spectral image can be of helpful to decrease speckles and identify linear road from flat water surface. As example, the data fusion and road extraction from the ERS-2 SAR image and Landsat ETM+, as well as RASARSAT-1 SAR image and Landsat ETM+, in Shanghai area are applied.

## 1. INTRODUCTION

Semi-automatic or automatic road detection from remotely sensed images in dense urban area is greatly helpful of urban transportation mapping, planning and management and in city GIS database etc.

During recent two decades, some approaches for automatic or semiautomatic detection of road from the optic or microwave radar images have been developed. These approaches usually take two steps: extracting possible road candidates, and linking road candidates. The first step is based on classification of remote sensing image (Dell *et al.*, 2001; Shackelford *et al.*, 2003) and conventional edge or line detection (Touzi *et al.*, 1988; Tupin *et al.*, 1998). It is most likely suitable to visible or infrared images with high spatial resolution and spectral resolution. There have been many approaches to linking the road candidates (Baumgartner *et al.*, 1999; Burns *et al.*, 1986; Jeon *et al.*, 2002).

However, it is well known that remote sensing of multiple sensors, e.g. at visible, infrared, and microwave frequencies, presents varying views on the geometries and spectrum reflectance of roads because of their different measuring physics. An infrared image may show rich spectral information, but is lack of sensitivity to mistakes of different spectrum for the same object and the same spectral for different objects. On the other hand, the multiplicative speckles in microwave radar image and, especially, complicated distribution of various objects in the urban area make the automatic road detection more difficult. Therefore, road information retrieval from a single sensor's data is always restrictive. And data fusion of multiple sensors may be a new tool to retrieve more accurate and richer road information in remote sensing applications.

In this paper, a semiautomatic method is developed based on the level set method for application to urban road extraction from multi-spectral and microwave radar remote sensing images. At first, the fast marching method of level set (LS-FM) is introduced briefly, which will play as a tool to fuse different image features for road extraction. Then different methods are applied to the extraction of road features from multi-spectral and microwave radar images respectively. A new iteration difference algorithm is proposed to calculate the spectral difference of objects in multi-spectral remote sensing image. After that, the speed function for LS-FM algorithm is defined with the features extracted from both multi-spectral image and microwave radar image. In this way, radar remote sensing image can make up road breaks due to shadowing of high building or tree canopy in multi-spectral image, while multi-spectral image can be of helpful to decrease speckles and identify linear road from flat water surface.

As example, the data fusion and road extraction from the ERS-2 SAR image and Landsat ETM+, as well as RASARSAT-1 SAR image and Landsat ETM+, in Shanghai area are applied.

## 2. LEVEL SET AND FAST MARCHING ALGORITHM

Level Set (LS) method was proposed by Osher and Sethian in 1989. And the basic idea of it is to present the closed plane curve implicitly as the level set of a two-dimensional surface function. And with the surface evolution of LS function, the curve evolution can be traced implicitly (Sethian, 1999).

Fast Marching (FM) is the fastest algorithm in LS method (Sethian, 1996). Supposed that the speed of the curve is always positive and  $T_{i,j}$  is the time the curve passing pixel  $(i, j)$ , the

---

\* Corresponding author.

evolution of the curve can be traced by its evolution time  $T$ , satisfying the following function.

$$|\tilde{N}T|F = 1, \quad (F > 0) \quad (1)$$

function (1) is one of Eikonal functions. It should be solved numerically due to the fact that it is difficult to be solved analytically. Rouy *et al.* proposed a very convenient upwind difference method (Rouy *et al.*, 1992), in which solving function (1) is equivalent to solving the following quadratic function:

$$\left[ \max(D_{ij}^+T, -D_{ij}^+T, 0)^2 + \max(D_{ij}^-T, -D_{ij}^-T, 0)^2 \right]^{\frac{1}{2}} = \frac{1}{F_{ij}} \quad (2)$$

where  $D_{ij}^{+x}T$  = the forward difference of  $T_{i,j}$  along  $x$  direction  
 $D_{ij}^{+y}T$  = the forward difference of  $T_{i,j}$  along  $y$  direction  
 $D_{ij}^{-x}T$  = the backward difference of  $T_{i,j}$  along  $x$  direction  
 $D_{ij}^{-y}T$  = the backward difference of  $T_{i,j}$  along  $y$  direction

The solving of function (2) not only requires the time  $T_{i,j}$  to be known, but also requires the speed function  $F$  determined by the image features to be monotonely decreasing function (Caselles *et al.*,1997). The time  $T_{i,j}$  in LS-FM algorithm can be updated with the inserting, deleting and sorting operations of the minimum heap structure (Sethian,1996a).

### 3. FEATURES EXTRACTION FROM REMOTE SENSING IMAGES

#### 3.1 Features Extraction from Multi-spectral Image

Both spectral and texture features are extracted from multi-spectral image for road detection. To make full use of the spectral information of road in multi-spectral remote sensing images and removing redundant information, three bands with close digital number to road but big digital number to other objects were selected to extract road from multi-spectral images with the following iterative difference algorithm:

$$\left. \begin{aligned} R^{n+1} &= |R^n - G^n| \\ G^{n+1} &= |G^n - B^n| \\ B^{n+1} &= |R^{n+1} - G^{n+1}| \\ S^{n+1} &= (R^{n+1} + G^{n+1} + B^{n+1})/3 \end{aligned} \right\} \quad (3)$$

where  $n$  = the iteration times

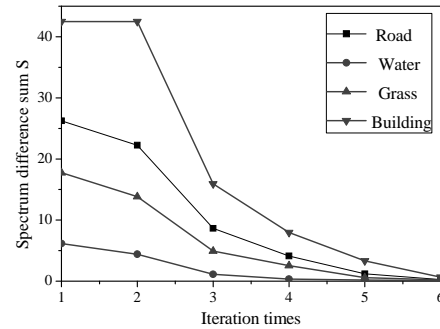


Figure 1. Relationship between S and iteration times for three bands data of different objects

Figure 1 shows the summary  $S$  of the spectral difference for different objects in the three bands after  $n$  iterations. It can be seen that there are obvious difference between road and other objects. And the higher the reflectivity of the object is, the bigger the  $S$  is. Only after 5 times of iteration,  $S$  of the object with lower reflectivity is going to zero while  $S$  of the object with higher reflectivity is still greater than zero. Thus, the contrast between road and grassland or water is enhanced and this presents a convenient way to recognize the road from them. The texture information of multi-spectral remote sensing image is presented with the entropy value calculated from its grey-level co-occurrence matrix (Haralick *et al.*,1973; Anys *et al.*,1994).

#### 3.2 Features Extraction from Microwave Remote Sensing Image

Spatial auto-correlation scales of microwave radar remote sensing image is calculated with the multi-layer and multi-scale Getis algorithm (Jin,2005; Yan *et al.*,2006). The distribution of the best spatial scale is used to present the cluster of the pixel values. And it is useful for the road extraction from the microwave radar remote sensing images due to the fact that the road often appears black in the images resulting from its low backscattering.

### 4. SPEED FUNCTION DEFINITION IN LS-FM ALGORITHM

The speed function in LS-FM algorithm is defined with different functions founded with different image features extracted above as well as the backscattering feature of microwave radar image. As for the spectral feature of multi-spectral image, texture and backscattering features of SAR image, the following function is used:

$$\left. \begin{aligned} R_x^f(i, j) &= \frac{X_0^f}{X^f(i, j)} \\ E_R^f(i, j) &= \exp\left(-\frac{1}{\sqrt{\alpha}}(R_x^f(i, j))^\beta\right) \end{aligned} \right\} \quad (4)$$

where  $f$  = spectral and texture features of multi-spectral images,  
 backscattering feature of radar image  
 $X_0^f$  = spectral and texture features of multi-spectral images,  
 backscattering feature of radar image for the seed point  
 $X^f(i, j)$  = spectral and texture features of multi-spectral images,  
 backscattering feature of radar image for pixel  $(i, j)$   
 $\alpha, \beta$  = constants smaller than 1

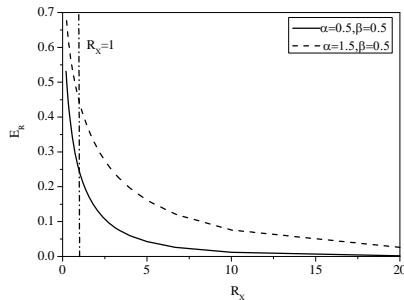


Figure 2.  $E_R$  vs.  $R_X$  with different  $\alpha$

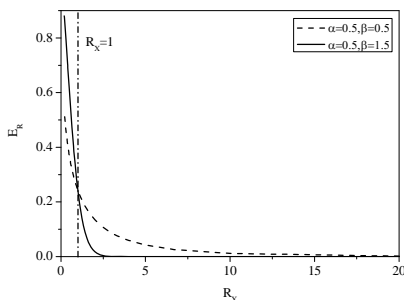


Figure 3.  $E_R$  vs.  $R_X$  with different  $\beta$

It can be seen from Figure 2 and 3 that  $E_R$  decreases monotonely with the increasing of  $R_X$ . When  $R_X > 1$ , that is,  $X_0 > X(i, j)$ ,  $E_R$  is going to 0 fastly. Otherwise,  $E_R$  will be larger value. When both  $\alpha$  and  $\beta$  are smaller than 1,  $E_R$  of all features will be closer to the medium value of the road in the image.

But when applying function (4) to the spatial auto-correlation scale of SAR remote sensing image, we failed to get the desired result. It may be due to the range of the spatial auto-correlation scale covers only the integers from -6 to 6. Therefore, the following function is used in the speed function for this feature.

$$\left. \begin{aligned} D_x(i, j) &= X_0 - X(i, j) \\ E_D(i, j) &= \exp(-a \times |D_x(i, j)|) \end{aligned} \right\} \quad (5)$$

where  $X_0$  = the spatial autocorrelation scale of the seed point  
 $X(i, j)$  = the spatial autocorrelation scale of pixel  $(i, j)$   
 $a$  = constant smaller than 1

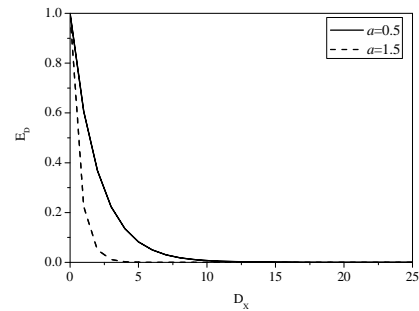


Figure 4.  $E_D$  vs.  $D_X$  with different  $a$

It can be seen from Figure 4 that  $E_D$  is decreasing monotonely with the increasing of  $D_X$ , when  $D_X = 0$ , that is  $X(i, j) = X_0$ ,  $E_D$  will be the maximum.

Finally, the speed function is defined by the following formula:

$$F = E_R^S \times E_R^T \times E_R^A \times E_D \quad (6)$$

where  $S$  = the spectral feature of multi-spectral images  
 $T$  = the texture feature of multi-spectral images  
 $A$  = the backscattering feature of radar image

By taking function (6) to function (2), it is easy to calculate  $T_{i,j}$ , the time when the surface passes the pixel  $(i, j)$  according to the methods proposed by Sethian and Telea (Sethian,1996; Telea,2004). And then, the edge of the road is obtained.

It is conducive to enhance the road information of the image if all the extracted features are formed in the speed function with equation (5). But the non-road objects will be enhanced at the same time. And if the road is incontinuous in one feature, it can't be made up by other features in which the road is continuous. Function (4) makes the road in all features to be the medium value and non-road objects to be bigger or smaller values depending on their difference to the road. If there is one of features extracted satisfies that the ratio between road and non-road is bigger, it will be smaller in function (6) while road will be bigger. For example, house has bigger value in the spectral feature extracted from the multi-spectral image, but it will be zero in the texture feature extracted from the same image because of its big and flat roof. Although grassland has big values in the texture feature of the multi-spectral image, it will be zero in its spectral feature. Road can be distinguished from linear water in the multi-spectral image with the spectral feature of it although they are similar to each other in the microwave radar image. Therefore, function (6) is proved to be a good way to enhance the road information with the combination of different features from both microwave radar and multi-spectral images.

## 5. EXAMPLE

### 5.1 Road Extraction with Fusion of ERS-2 SAR and Landsat ETM + Images

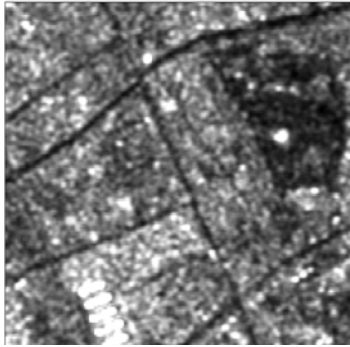


Figure 5. ERS-2 SAR image of Shanghai, China



Figure 6. Landsat ETM+531 image of Shanghai, China

An ERS-2 SAR data (5.3GHz, VV polarization, spatial resolution 12.5m) on the April 9, 2002 and a Landsat ETM+ data (spatial resolution is 30m) on the November 27, 2002 over the Central Park of Shanghai Pudong District, China are taken as an example. The ERS-2 SAR image is shown in Figure 5 and the combination of band 1, 3 and 5 of Landsat ETM+ image is shown in Figure 6. It can be seen that it is difficult to distinguish the road from linear water at the top right of the microwave radar image.

The crossroads in the upper and lower left of Figure 6 present that some roads are broken by the shadows of the vegetation and house surrounding them in the multi-spectral image. Besides, the fact that there are some other objects whose spectral features are similar to the road also makes it difficult to extract the road from only multi-spectral image.

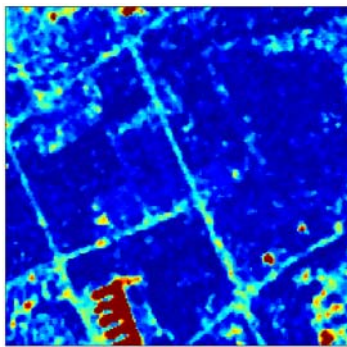


Figure 7. The result of the iteration difference for Landsat ETM+531 image

Figure 7 presents the spectral feature extracted from the multi-spectral image with the iterative difference method of this paper. It shows that the value of the road and house in the lower left of the image is larger than other objects and makes them easy to be extracted from the images.

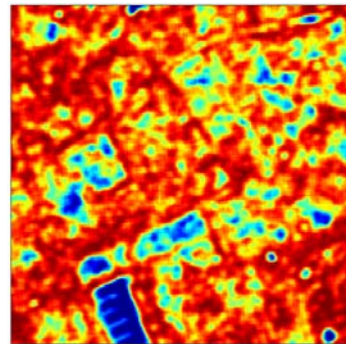


Figure 8. Texture features extracted from Landsat ETM+ image

Figure 8 shows the texture extracted from the entropy of the gray-level co-occurrence matrix of the multi-spectral image. The house with big and flat surface presents smaller value while the road edge and the region with abundant texture present larger values.

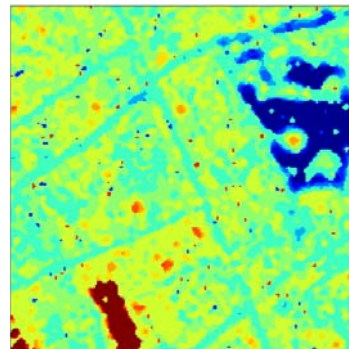


Figure 9. Distribution of spatial size for ERS-2 SAR

Figure 9 is the spatial auto-correlation scale of ERS-2 SAR image calculated with multi-layer and multi-scale Getis spatial autocorrelation method. The red or yellow color in the image shows the positive spatial auto-correlation scale, resulting from the cluster of the buildings. Green or blue color shows negative spatial auto-correlation, resulting from the cluster of such objects as grassland, flat surface, wide road or river with smaller backscattering characteristics.

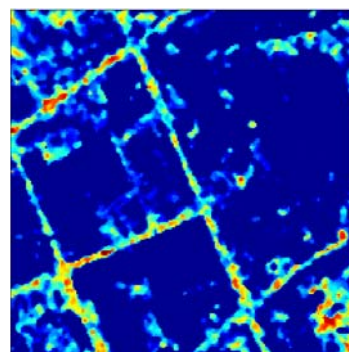


Figure 10. Fusion image of Landsat ETM+ and ERS-2 SAR

Figure 10 is the fusion result of extracted features with function (6), in which the road is better enhanced. The comparison between it and images of Figure 5-9 shows that the fusion result not only decreases the interference of linear water to road, but also makes the broken road in the upper left, middle of the left and lower right continuous by taking both advantage of microwave radar and multi-spectral images.

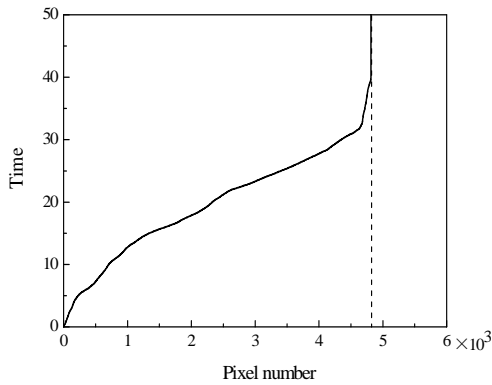


Figure 11. Time trend got from LS-FM algorithm

The time evolution of LS-FM algorithm is shown in Figure 11. It can be seen that the time increases gradually. When the evolution passes about 4800 pixels, the time is going to be a very great value and the road edge is arrived.

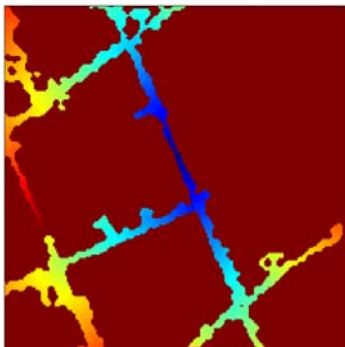


Figure 12. Time evolution image got from LS-FM algorithm

Figure 12 is the final time evolution result. Colour from blue to red indicates the change of the time from small to large, and the deep red color shows the non-road information with large time value. It can be seen that the LS-FM algorithm can better overcome the interference of non-road objects in Figure 10 and extract the road. But because of the existence of the objects similar to road, the road extracted has some irregular swells.

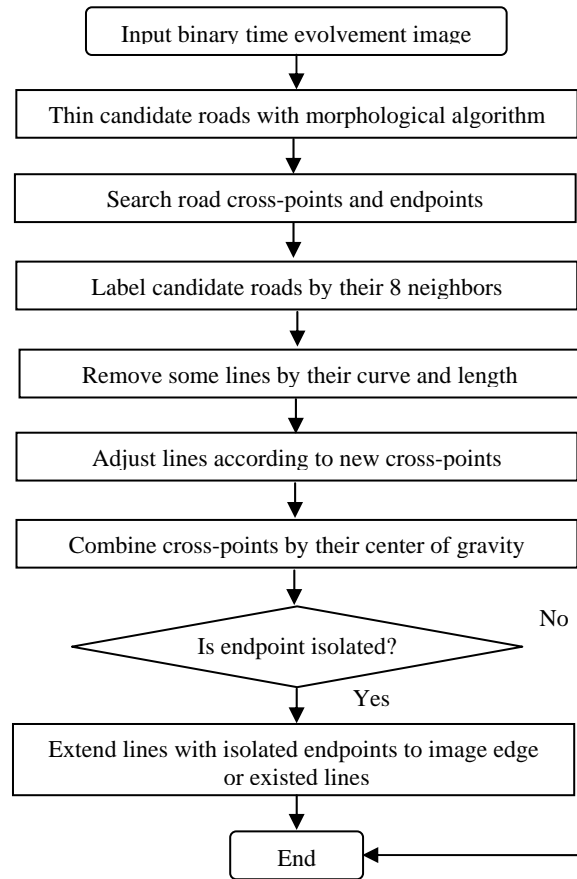


Figure 13. The flow chart for road connection

In order to get one pixel width road, the result in Figure 12 is processed with methods in Figure 13.

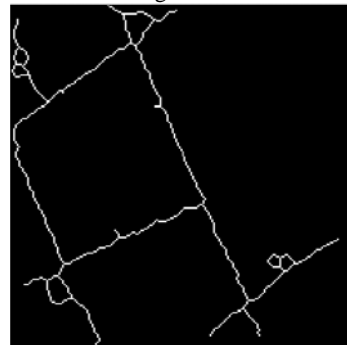


Figure 14. The thinned time evolution image

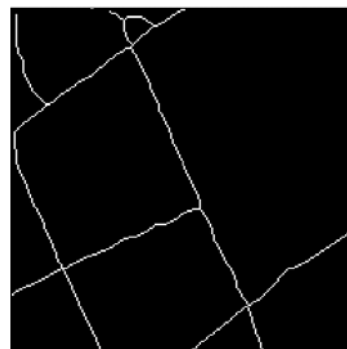


Figure 15. The extracted road image

Figure 14 presents the thinned candidate road with morphological algorithm. The comparison between the final detected road in Figure 15 with the original microwave radar or multi-spectral image shows that the road extracted is quite satisfactory.

## 5.2 Road Extraction with Fusion of Radarsat-1 SAR and Landsat ETM+

A RADARSAT-1 SAR data (5.3GHz, HH polarization, spatial resolution 6.25m) on the November 18, 2002 and the corresponding Landsat ETM+ data with the same characteristics as that in Figure 6 are also taken as an example. They are shown in Figure 16 and Figure 17. Figure 18 presents the road extracted with method of this paper, which is also very satisfactory.



Figure 16. Radarsat-1 SAR image of Shanghai, China



Figure 17. Landsat ETM+531 image of Shanghai, China

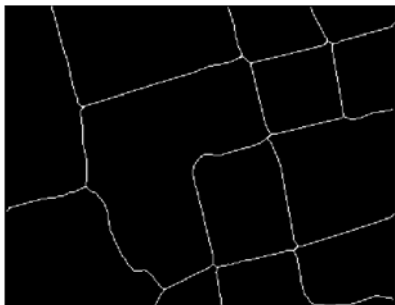


Figure 18. The extracted road image

## 6. CONCLUSION

In this paper, the LS-FM algorithm is developed to fuse the multi-spectral and microwave radar remote sensing images to

extract road from complex urban areas. It is applied to the data fusion and road extraction from the ERS-2 SAR image and Landsat ETM+, as well as RADARSAT-1 SAR image and ETM+, in Shanghai area, China.

(1) The iteration difference algorithm is a good way to present the spectral difference of different objects in multi-spectral images with only several iterations, especially those with big difference in reflectivity.

(2) Fused images from multiple sensors, such as infrared ETM+ and microwave radar images, can yield satisfactory road extraction of complex terrain surfaces. Using the LS-FM and multiple sensor's fused data, their advantages can be synthesized together to make better road extraction

## ACKNOWLEDGEMENTS

This work was supported by China State Major Basic Research Project (2005CB724204), the National Natural Science Foundation of China (40701020).

## REFERENCES

- Anys H., Bannari A., He D. C., Morin D.,1994. Texture analysis for the mapping of urban areas using airborne MEIS-II images. In: *Proceedings of the First International Airborne Remote Sensing Conference and Exhibition*, Strasbourg, France, Vol.3, pp: 231-245.
- Baumgartner A., Steger C., Mayer H., Eckstein W., Ebner H.,1999. Automatic road extraction based on multi scale, grouping, and context. *Photogrammetric Engineering and Remote Sensing*, Vol. 65, pp: 777-785.
- Burns J., Hanson A., Riseman E.,1986. Extracting straight lines. *IEEE Transactions on Pattern Analysis and Machine Intelligent*, pp: 425-455.
- Caselles V., Kimmer R., Sapiro G.,1997. Geodesic active contours. *International Journal of Computer Vision*, 22(1), pp: 61-79.
- Dell A. F., Gamba P.,2001. Detection of urban structures in SAR images by robust fuzzy clustering algorithms: the example of street tracking. *IEEE Transactions on Geoscience and Remote Sensing*, Vol. 39, pp: 2287-2297.
- Haralick R. M., Shanmugan K., Dinstein I.,1973. Textural features for image classification. *IEEE Transactions on Systems, Man, and Cybernetics*, 3(6), pp: 610-621.
- Jeon K., Jang J. H., Hong K. S.,2002. Road detection in spaceborne SAR images using a genetic algorithm. *IEEE Transactions on Geoscience and Remote Sensing*, Vol. 40, 22-29.
- Jin Y. Q.,2005. *Theory and Approach of Information Retrievals from Electromagnetic Scattering and Remote Sensing*. Germany: Springer, Chapter 3.
- Rouy E., Tourin A.,1992. A viscosity solutions approach to shape-from-shading. *SIAM Journal on Numerical Analysis*, 29(3), pp: 867-884.

Sethian J. A.,1999. *Level Set Methods and Fast Marching Methods*. Cambridge: Cambridge University Press, pp: 3-76.

Sethian J. A.,1996. *A Review of the Theory, Algorithms, and Applications of Level Set Methods for Propagating Interfaces*. Acta Numerica, Cambridge University Press, pp: 487-499.

Shackelford A. K., Davis C. H.,2003. Urban road network extraction from high-resolution multispectral data. In: *2nd GRSS/ISPRS Joint Workshop on Remote Sensing and Data Fusion over Urban Areas (URBAN 2003)*, Berlin, Technical University of Berlin, pp. 142-146.

Telea A.,2004. An Image inpainting technique based on the fast marching method. *Journal of Graphics Tools*, 9(1), PP: 25-36.

Touzi R., Lopes A., Bousquet P.,1988. A statistical and geometrical edge detector for SAR images. *IEEE Transactions on Geoscience and Remote Sensing*, Vol. 26, pp: 764-773.

Tupin F., Maitre H., Mangin J. F., Nicolas J. M., Pechersky E., 1998. Detection of linear features in SAR images: Application to road network extraction. *IEEE Transactions on Geoscience and Remote Sensing*, Vol. 36, pp: 434-453.

Yan F. H., Jin Y. Q.,2006. Spatial Auto-correlation of Characteristic Parameters in Remotely Sensed Image Using Optimal Multi-scale Getis Statistic. *Journal of Image and Graphics*, 11(2), PP: 191-196.

